MLCK regulates Schwann cell cytoskeletal organization, differentiation and myelination

Ellen M. Leitman[1,*], Ambika Tewari[1,*], Meryl Horn[1], Mateusz Urbanski[1,2], Evangelos Damanakis[1], Steven Einheber[3], James L. Salzer[4], Primal de Lanerolle[5] and Carmen V. Melendez-Vasquez[1,‡]

[1]Department of Biological Sciences, Hunter College, City University of New York, New York, NY 10065, USA
[2]The Graduate Center, City University of New York, New York, NY 10016, USA
[3]School of Health Sciences, Hunter College, City University of New York, New York, NY 10010, USA
[4]Department of Cell Biology and Smilow Neuroscience Program, New York University School of Medicine, New York, NY 10016, USA
[5]Department of Physiology and Biophysics, University of Illinois at Chicago, Chicago, IL 60612, USA

*These authors contributed equally to this work
‡Author for correspondence (melendez@genectr.hunter.cuny.edu)

Accepted 4 July 2011
Journal of Cell Science 124, 3784–3796

doi: 10.1242/jcs.080200

Summary

Signaling through cyclic AMP (cAMP) has been implicated in the regulation of Schwann cell (SC) proliferation and differentiation. In quiescent SCs, elevation of cAMP promotes the expression of proteins associated with myelination such as Krox-20 and P0, and downregulation of markers associated with the non-myelinating SC phenotype. We have previously shown that the motor protein myosin II is required for the establishment of normal SC–axon interactions, differentiation and myelination, however, the mechanisms behind these effects are unknown. Here we report that the levels and activity of myosin light chain kinase (MLCK), an enzyme that regulates MLC phosphorylation in non-muscle cells, are dramatically downregulated in SCs after cAMP treatment, in a similar pattern to that of c-Jun, a known inhibitor of myelination. Knockdown of MLCK in SCs mimics the effect of cAMP elevation, inducing plasma membrane expansion and expression of Krox-20 and myelin proteins. Despite activation of myelin gene transcription these cells fail to make compact myelin when placed in contact with axons. Our data indicate that myosin II activity is differentially regulated at various stages during myelination and that in the absence of MLCK the processes of SC differentiation and compact myelin assembly are uncoupled.

Key words: Schwann cell, MLCK, Myosin II, Myelination

Introduction

The development of Schwann cells (SCs) into fully mature myelin-forming cells relies on sustained axon-derived signals. Before myelination, SCs undergo extensive remodeling of their cytoskeleton and mode of association with the axon. In a process known as axonal sorting, axons selected for myelination are first segregated in a 1:1 association with the SCs. Myelination then proceeds by the progressive extension and wrapping of the inner plasma membrane around the axon (Bunge et al., 1989). It has been shown that the expression levels of axonal NRG1 type III provides a crucial signal for axonal sorting and the induction of the myelinating phenotype in SCs (Michailov et al., 2004; Taveggia et al., 2005). Axonal signals also activate expression of transcription factors, such as Oct-6 (also known as POU domain, class 3, transcription factor 1, Pou3f1) and Krox-20 (also known as early growth response protein 2, EGR-2) that trigger the initiation of the myelination program in SCs. Elevation of cyclic adenosine monophosphate (cAMP) can mimic axonal contact in vitro and stimulate SC differentiation (Morgan et al., 1991; Sobue and Pleasure, 1984). More recently, signaling through Gpr126, a G-protein-coupled receptor has been shown to drive SC differentiation by elevation of cAMP levels and stimulation of Oct-6 expression (Monk et al., 2009).

Although several studies have implicated the actin cytoskeleton and members of the small Rho-GTPase family in process extension, axonal segregation, differentiation and myelin formation by SCs (Benninger et al., 2007; Nodari et al., 2007; Pereira et al., 2009), little is known about how the pathways activated in SCs, by axonal signals, direct the morphogenetic changes associated with their entry into the myelinating program. We have previously shown that myosin II, a protein that regulates actin cytoskeleton dynamics plays a key role during SC development, and that downregulation or inhibition of its activity impairs SC differentiation and myelination (Wang et al., 2008). In non-muscle cells, myosin II is activated by phosphorylation of myosin light chain (MLC) (Adelstein and Conti, 1975). Rho kinases (ROCK) regulate the activity of myosin II (Totsukawa et al., 2004; Totsukawa et al., 2000) and inhibitors of ROCK have previously been shown to downregulate MLC phosphorylation and affect the coordinated wrapping of SCs around the axons and their domain organization (Melendez-Vasquez et al., 2004). Non-muscle myosin II is also directly regulated by myosin light chain kinase (MLCK), a Ca^{2+}/calmodulin-activated kinase whose only known target is MLC (Gallagher et al., 1997). Previous studies have demonstrated that changes in MLC phosphorylation and MLCK activity can regulate cell differentiation (Chang et al., 2007; Chen et al., 2007; Ihnatovych et al., 2007; Maddala et al., 2007). In this study we examined the distribution and regulation of MLCK in SCs and found that after treatment with cAMP analogues, the levels and

activity of MLCK are downregulated, in a manner similar to that reported for markers of non-myelinating immature SCs. Furthermore, downregulating MLCK protein levels in SCs using short hairpin RNA (shRNA) simulates the effects of cAMP treatment and results in cell-cycle arrest, changes in SC morphology and upregulation of markers of the pro-myelinating program. Despite activation of myelin gene transcription and differentiation, we found that SCs lacking MLCK activity do not myelinate normally when placed in coculture with axons. In the absence of shMLCK activity, most SCs did not complete radial sorting and made thinner and fewer compact myelin segments. shMLCK-treated SCs also exhibit abnormalities in protein trafficking indicating that MLCK and/or myosin II activity might be required at different levels during myelination. These results provide novel evidence that regulation of actin cytoskeleton dynamics by myosin II is crucial for the induction of SC differentiation and myelin formation and that these processes can be dissociated in vitro by downregulation of MLCK in SCs.

Results

MLCK is highly expressed in the nucleus of SCs and is downregulated during myelination

We examined the distribution and expression of MLCK in SCs in vitro and in vivo. Non-muscle cells express at least two different isoforms of MLCK with apparent molecular masses of 200–220 kDa (long) and 130–155 kDa (short). These proteins are products of a single gene and only differ by the presence of a N-terminal extension in the long isoform, containing multiple sites for protein–protein interactions and binding to actin (Gallagher et al., 1997). We have found that although both isoforms are detected in SCs, the shorter isoform, with an apparent molecular mass of 155 kDa predominates (Fig. 1B,D).

Staining with several affinity-purified MLCK antibodies (de Lanerolle et al., 1981; de Lanerolle et al., 1987) showed that in cultured SCs, MLCK is mostly concentrated in the perinuclear cytoplasmic region and cell nucleus (Fig. 1A). The specificity of the nuclear staining was directly confirmed by pre-absorbing the antibodies with purified MLCK from chicken gizzard (data not shown) and by carrying out subcellular fractionation (Fig. 1B). Similarly, SCs in non-myelinating cocultures exhibited strong nuclear MLCK staining that decreased as cultures were induced to myelinate (Fig. 1C). This finding was confirmed by western blotting of SCs, dorsal root ganglion (DRG) neurons and myelinating cocultures lysates (Fig. 1D). DRG neurons also expressed low levels of a different MLCK isoform with an apparent molecular mass of 135–140 kDa. Staining in sciatic nerves showed a more complex pattern because endothelial cells and axons also expressed substantial levels of MLCK (Fig. 1E), but nuclear staining was also evident and considerably reduced in Krox-20-positive (Krox-20^{+}) myelinating SCs. Taken together these data suggest that, in addition to its role as a cytoskeletal regulator, MLCK might have an unknown function in the nucleus of glial cells.

Elevation of cAMP in SCs downregulates MLCK and MLC phosphorylation

In order to understand the mechanisms regulating myosin II activity we decided to study the effects of cAMP treatment on MLCK expression and MLC phosphorylation in SCs. Elevation of cAMP in SCs is thought to mimic early axonal signals that are crucial for the development of the myelinating phenotype. Primary rat SCs were expanded in medium containing 10% serum and growth factors (4 μM forskolin and 5 ng/ml of recombinant human neuregulin-1-β1; rhNRG1-β1) until confluent. At this point growth factors were removed and cultures were maintained in 10% serum for a minimum of 3 days before the experiment. SCs cultures were either serum-starved or switched to defined medium overnight (t=0) before treatment with 1 mM dibutyryl cyclic cAMP (db-cAMP; a membrane-permeable derivative of cyclic AMP) for 30 minutes to 72 hours (Fig. 2A).

As expected, elevation of cAMP levels induced upregulation of cell cycle inhibitor p27^{Kip} (Larocque et al., 2009) as well as that of pro-myelinating transcription factors (Oct-6 and Krox-20) and myelin proteins (MAG and P0) (Monuki et al., 1989; Parkinson et al., 2004), while reducing the expression of c-Jun, a negative regulator of myelination (Parkinson et al., 2008), and other markers of non-myelinating SCs such as p75 and N-cadherin (Monje et al., 2009; Morgan et al., 1991). Surprisingly, treatment with cAMP dramatically downregulated the expression of MLCK and the level of phosphorylated MLC (MLC-*P*), indicating an overall reduction of myosin II activity in pro-myelinating SCs. Levels of Rho-associated kinases (ROCK1, ROCK2) and myosin phosphatase (MYPT1), which also regulate MLC phosphorylation were not affected by cAMP treatment, whereas levels of total MLC2 dropped only after 72 hours (Fig 2A). Interestingly, we also observed an increase in MLCK phosphorylation following cAMP treatment (Fig. 2A), which is consistent with the demonstration that phosphorylation by cyclic AMP-dependent protein kinase inhibits MLCK activity (de Lanerolle et al., 1984).

Staining of SCs also confirmed a marked reduction in MLCK nuclear staining following treatment with cAMP and upregulation of Krox-20 expression (Fig. 2B). These cells also upregulated expression of myelin proteins such as P0 and MAG (Fig 2A,D), and showed dramatic changes in actin cytoskeleton organization (Fig. 2C,D) including loss of thick contractile stress fibers and extensive cell spreading, resulting in bigger cells with a flattened morphology (Fig. 2D).

Time-lapse microscopy of SCs treated with cAMP during the first 24 hours (supplementary material Movie 1) revealed dynamic cytoskeleton rearrangements including the appearance of many long processes, the rounding of the cell nucleus and cytoplasm collapse, followed by the extension of flat membrane sheets. Collectively these data suggest that upon treatment with cAMP and induction of the myelination program, there is a reduction of MLCK levels and myosin II phosphorylation accompanied by actin cytoskeleton remodeling as SCs change their shape and extend sheath-like membrane sheets.

Downregulation of MLCK by shRNA mimics the effects of cAMP elevation in SCs

To test whether downregulation of MLCK activity is sufficient to induce changes associated with the pro-myelinating SCs phenotype, SCs cultures were infected with lentivirus expressing short hairpin RNA (shRNA) targeting MLCK (shMLCK). As controls, SCs cultures were infected with lentivirus expressing non-targeting shRNA (shCTRL). After infection, effective knockdown of MLCK (60-80% reduction of the relative intensity of the protein band) was confirmed by western blotting (Fig. 3B), which also showed a reduction of MLC-*P* levels, thus indicating a reduction of MLCK activity. Surprisingly, knockdown of MLCK in SCs also resulted in the dramatic upregulation of markers associated with the

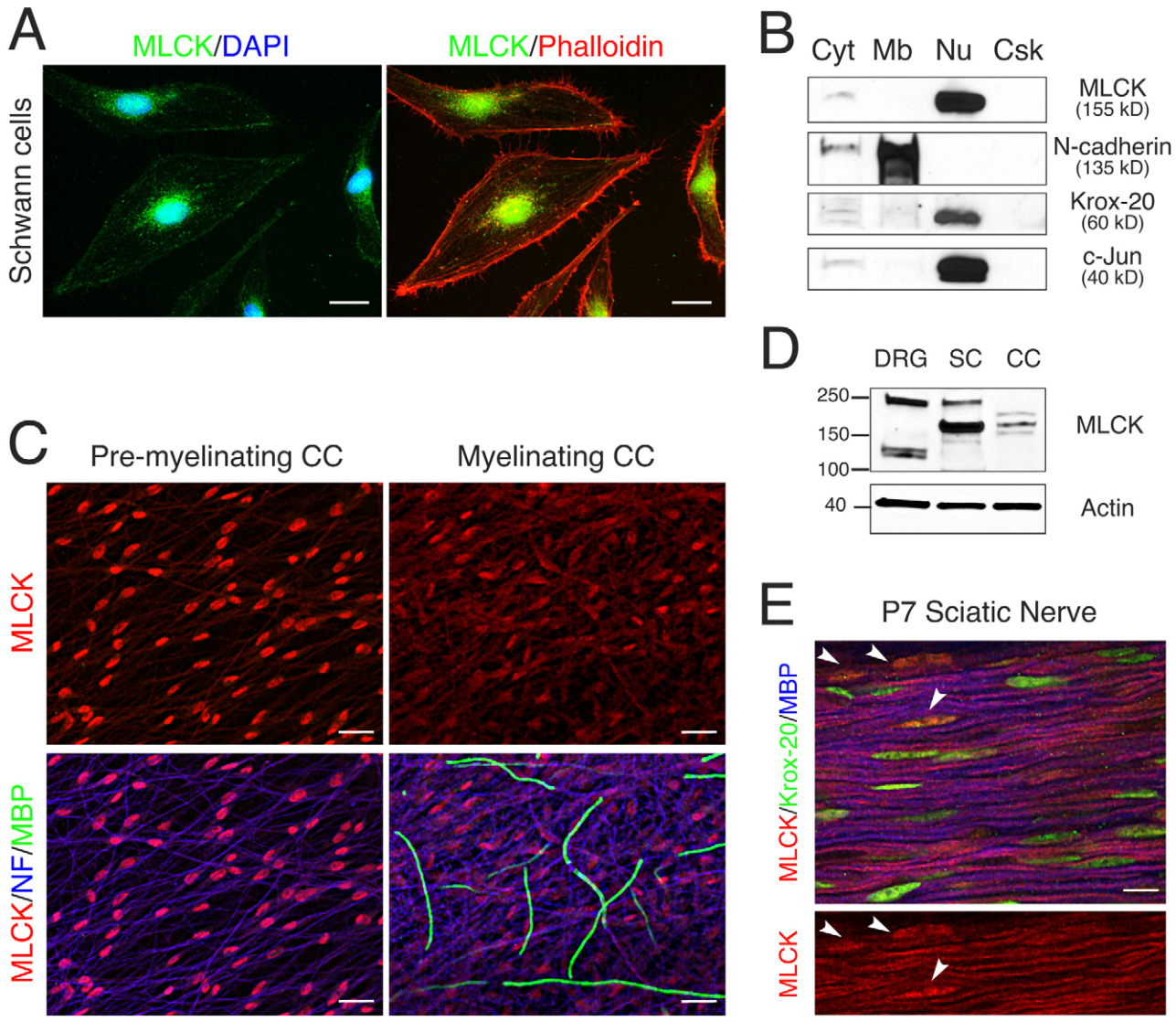

Fig. 1. Expression of MLCK in SCs in vitro and in vivo. (**A**) Primary cultures of rat SCs demonstrate strong expression of MLCK (green) in the nucleus and perinuclear cytoplasm, and weaker staining in the membrane and stress fibers where it colocalizes with actin (red). Scale bars: 15 μm. (**B**) Western blots of SC lysates after subcellular fractionation, confirming enrichment of MLCK in the nuclear fraction (Nu). A weak MLCK signal was also detected in the cytoplasmic fraction (Cyt), but none was detected in either the membrane (Mb) or cytoskeletal fraction (Csk). N-cadherin, and Krox-20 and c-Jun were used as markers for the membrane and nuclear fractions, respectively. (**C**) SC–neuron cocultures maintained in either pre-myelinating or myelinating conditions, stained with antibodies to MLCK (red), neurofilament (blue) and MBP (green). Strong MLCK staining is seen in the nucleus of pre-myelinating SCs. The intensity of the staining decreases considerably in myelinating cultures. Weak axonal staining for MLCK is also apparent in these cultures. Scale bars: 25 μm. (**D**) Western blot of SCs, DRG and 14-day myelinating coculture (CC) showing strong MLCK expression in SCs and weaker expression of a lower molecular mass isoform in DRG (overexposed lower panel). In myelinating cocultures, MLCK expression is downregulated. (**E**) Frozen section of P7 rat sciatic nerve stained with antibodies to MLCK (red), Krox-20 (green) and MBP (blue). MLCK is present in axons and in the nucleus of non-myelinating SCs (arrowheads) but not in Krox-20^{+} myelinating SCs. Scale bar: 10 μm.

activation of the myelination program, such as $p27^{Kip}$, Krox-20, P0, MAG and α-2 laminin chain; and decreased c-Jun expression (Fig. 3B). Immunostaining (Fig. 3A, lower panels) also confirmed a significant increase in the number of SCs expressing high levels of P0 protein in MLCK-knockdown cultures (shMLCK: 45±2.4% vs shCTRL: 2.7±0.5%; means ± s.e.m.; $P<0.0001$). These cells had a flattened process-bearing morphology with a rounder and enlarged nucleus (Fig. 3A, upper panels). These changes are consistent with those previously reported to occur in SCs after prolonged cAMP treatment (Monuki et al., 1989; Parkinson et al., 2004). Proliferation assays also showed a reduction in the percentage of $BrdU^{+}$ cells in cultures treated with shMLCK (9.5±0.5%) compared with controls (12.7±0.9%; means ± s.e.m.). Taken together these data suggest that downregulation of MLCK promotes cell-cycle exit in SCs and their entry into the pro-myelinating program, as well as dramatic changes in the organization of the SC cytoskeleton, which are comparable to those observed after treatment with cAMP analogues.

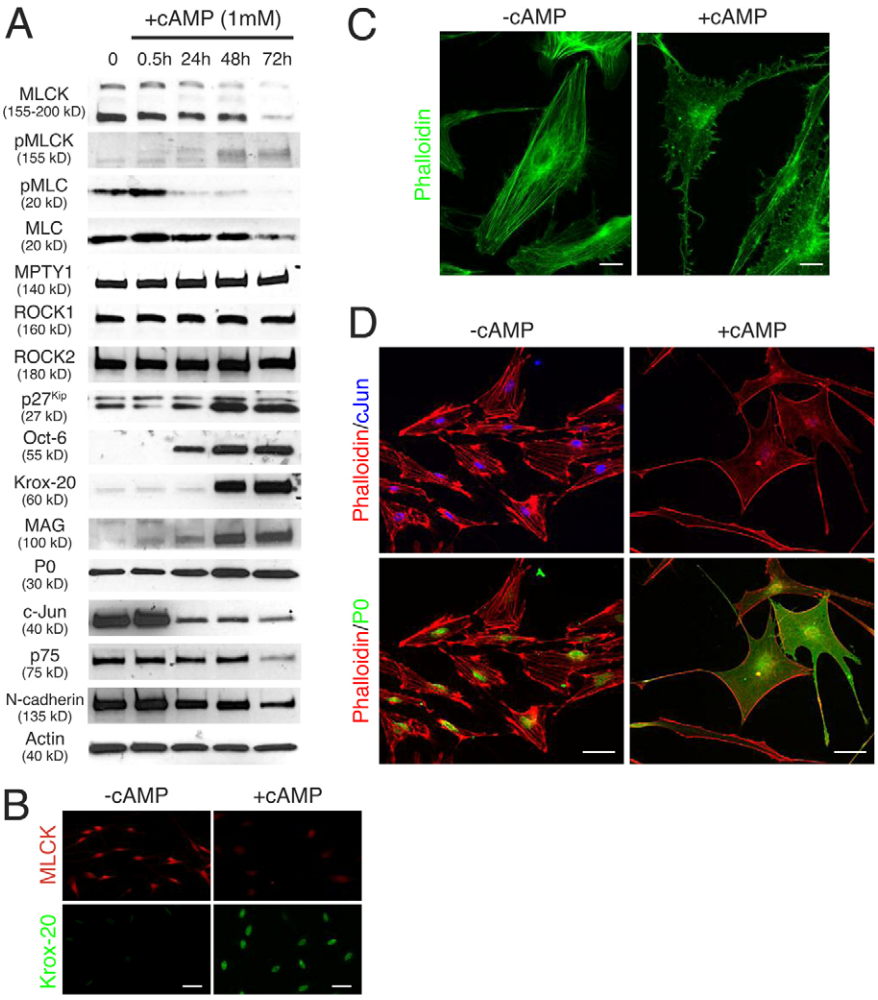

Fig. 2. Elevation of cAMP downregulates MLCK expression and activates the myelination program. (**A**) Western blots of SC cultures maintained in defined medium (t=0) and stimulated with 1 mM db-cAMP for 0.5–72 hours. Treatment with cAMP upregulates the expression of pro-myelinating transcription factors Oct-6 and Krox-20 and myelin proteins such as MAG and P0, and downregulates the expression of c-Jun, MLCK and phosphorylated MLC. There is also an increase in MLCK phosphorylation. (**B**) SC cultures were maintained in defined medium and stimulated for 48 hours with 1 mM db-cAMP. A striking decrease in MLCK nuclear staining (red) is observed after cAMP treatment, concomitant with an increase in Krox-20 expression (green). (**C**) Detail of the changes in the actin cytoskeleton organization after a 30-minute treatment with 1 mM db-cAMP. Scale bars: 10 μm. (**D**) SC cultures stained with antibodies to P0 (green), phalloidin-TRITC (red) and c-Jun (blue) before and after treatment with 1 mM db-cAMP for 72 hours. Loss of stress fibers and considerable cell expansion occurs in stimulated SCs together with upregulation of P0 expression and downregulation of c-Jun. Scale bars: 25 μm.

Increased phosphorylation of MLC affects SC morphology and partially prevents activation of the myelination program by cAMP

We next investigated whether upregulation of MLC-*P* levels prevents the changes in SCs morphology and differentiation induced by elevation of cAMP. To this end we infected SCs with lentiviral construct expressing shRNA against MYPT1, an enzyme that decreases myosin II activity by dephosphorylation of MLC (Kimura et al., 1996). As expected, knockdown of MYPT1 (66–80% reduction of the relative intensity of the protein band) in SCs resulted in increased levels of MLC-*P* in SCs (Fig. 3C,D). Unlike the changes observed after knockdown of MLCK and MLC-*P* downregulation (Fig. 3B), the expression levels of P0 and Krox-20 were not upregulated by MYPT1 knockdown (Fig. 3C). Next we examined whether the induction of the myelination program by cAMP was impaired in SCs treated with shMYPT1. We found that although downregulation of MLCK and c-Jun, as well as upregulation of Oct-6 by cAMP was unaffected by knockdown of MYPT1 (Fig. 3E), upregulation of Krox-20 was notably reduced (Fig. 3E). Of note, in SCs treated with shMYPT1 the level of MLC-*P* did not decrease after 24 hours of cAMP treatment, as occurred in control cultures (Fig. 3E). Immunofluorescence of cultures treated with shMYPT1, revealed the presence of cells with thick stress fibers and intense MLC-*P* staining (Fig. 3D). Upon treatment with cAMP, these cells did not upregulate P0 expression (Fig. 3F, upper panel). Similar results were obtained when SCs were infected with an adenovirus construct expressing a constitutive active form of MLCK (Ihnatovych et al., 2007) (supplementary material Fig. S1). Strong P0 expression and membrane expansion was consistently observed only in cells with low levels of MLC-*P*, which also lacked stress fibers (Fig. 3F, lower panel) and presumably did not have an efficient MYPT1 knockdown. Taken together these results suggest that although some transcriptional activation events triggered by cAMP are independent of MLC-*P* levels, the changes in the organization of the SC cytoskeleton that are associated with increased P0 protein expression and membrane expansion are correlated with lower levels of MLC-*P* and the loss of stress fibers.

Downregulation of MLCK in SCs impairs myelination in cocultures

In order to study the effects of MLCK knockdown in myelin formation, shMLCK-infected SCs were added to DRG neurons and allowed to proliferate for 3 days before changing the medium to one containing ascorbic acid to stimulate myelination. Inspection of cultures at this pre-myelinating stage showed that SCs infected with shMLCK elaborated very long and thin processes, which were not observed in control SCs (supplementary material Movie 2). Despite these morphological differences, SCs in shMLCK cultures

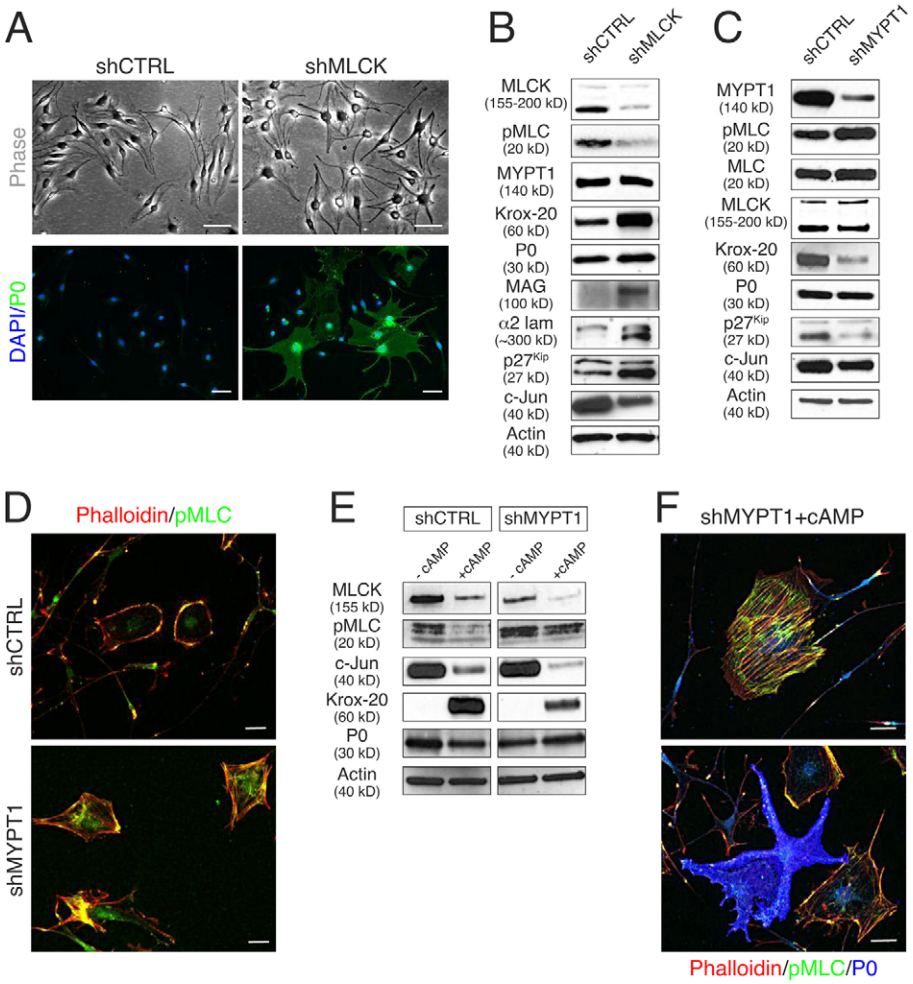

Fig. 3. Knockdown of MLCK in SCs activates the myelination program. (**A**) Primary cultures of rat SCs were infected with lentiviral constructs expressing non-targeting shRNA (shCTRL) or shRNA against MLCK (shMLCK). Upper panels: phase-contrast images showing striking morphological differences between these cultures. Lower panels: a dramatic upregulation of P0 expression (green) was observed in SC cultures treated with shMLCK compared with controls (shCTRL). Scale bars: 25 μm. (**B**) Western blots of SC cultures showing reduction of MLCK and MLC-*P* (pMLC) levels as well as activation of myelination program in SCs treated with shMLCK compared with shCTRL. (**C**) Western blots of SC cultures infected with non-targeting shRNA (shCTRL) or shRNA against myosin phosphatase 1 (shMYPT1). Increased levels of MLC-*P* are seen in shMYPT1-treated SCs, confirming knockdown of the phosphatase. No changes in P0 levels are observed whereas levels of Krox-20, c-Jun and $p27^{Kip}$ are decreased compared with control cultures. (**D**) SCs cultures showing increased level of MLC-*P* (green) and robust stress fiber formation in cultures treated with shMYPT1 compared with controls (shCTRL). Scale bars: 25 μm. (**E**) Western blots of control- and shMLCK-treated SC cultures before (−) and after (+) stimulation with 1 mM db-cAMP for 24 hours. In MYPT1-knockdown cultures, MLC-*P* levels remain high, although downregulation of MLCK and c-Jun and upregulation of Oct-6 after cAMP treatment appear unaffected; upregulation of Krox-20 was reduced compared with control cultures. (**F**) Immunofluorescence of SCs after 24 hours of 1 mM db-cAMP stimulation, showing a reverse correlation between the expression of P0 and the presence of high levels of MLC-*P*. Cells with high levels of MLC-*P* exhibit abundant stress fibers and lack P0 expression (upper panel); whereas cells expressing high levels of P0 lack stress fibers and have reduced expression of MLC-*P* (lower panel). Scale bars: 20 μm.

contacted and moved normally along the axons (supplementary material Movie 2) and expressed laminin (Fig. 4). Staining for c-Jun showed reduced expression of this non-myelinating transcription factor in shMLCK-treated SCs compared with control SCs at the same stage (Fig. 4). These results demonstrate that knockdown of MLCK did not impair the early association of SCs with axons and downregulated the expression of factors associated with the non-myelinating phenotype in pre-myelinating cultures.

After 2–3 weeks in myelinating conditions, we examined the cultures for myelin basic protein (MBP) expression as previously described (Wang et al., 2008). We found that cultures established with MLCK-deficient SCs exhibited a significant reduction in the number of MBP^{+} segments formed compared with controls (Fig. 5A). Quantification of three independent experiments (Fig. 5B) showed a reduction of 96% in the average number of MBP segments between shCTRL and shMLCK cultures (shCTRL: 70.6 ± 56 vs shMLCK: 2.3 ± 7.3; means $\pm$ s.e.m.; $P<0.0001$). Western blotting analysis (Fig. 5C) also confirmed a considerable reduction in MBP expression; however, expression of other markers such as Krox-20, P0 and MAG, albeit reduced, was still prominent (Fig. 5C). This observation was also confirmed by immunofluorescence staining that showed the presence of MAG^{+} (Fig. 5A) or $P0^{+}$ segments (Fig. 5D) in the absence of MBP expression. More importantly, despite the lack of MBP staining, substantial expression of Krox-20 was detected in shMLCK cultures (Fig. 5E). Thus, despite the fact that

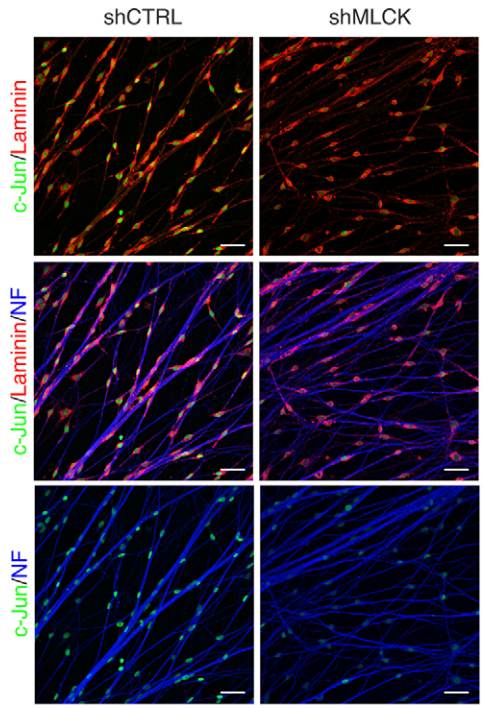

Fig. 4. Knockdown of MLCK in SCs does not prevent initial SCs–axon association. SCs infected with lentiviral constructs expressing non-targeting shRNA (shCTRL) or shRNA against MLCK (shMLCK) were seeded onto purified DRG neurons and allowed to proliferate for 3 days. Cultures were stained for laminin (red), c-Jun (green) and neurofilament (NF; blue). SCs (red) infected with shMLCK elaborate very thin and long processes, but they appear to contact and extend along the axons (blue). Expression of c-Jun is downregulated in shMLCK cultures compared with controls. Scale bars: 50 μm.

downregulation of MLCK in SCs activates the myelination program, when placed in cocultures with axons these cells are unable to form compact myelin.

Further evidence that knockdown of MLCK in SCs does not interfere with the activation of myelin gene transcription was provided by real-time PCR analysis (Fig. 6). Thus, mRNA levels for MAG, P0 and Krox-20 were significantly increased in cocultures established with shMLCK-treated SCs, whereas the expression of laminin α2, a marker of basal lamina assembly, was not affected by MLCK downregulation, at either the protein or mRNA level (Fig. 4C; Fig. 6). Only MBP mRNA was reduced in shMLCK cocultures especially during the first two weeks. However, by 21 days, MBP mRNA levels were comparable between control and MLCK-deficient cultures (Fig. 6), yet the myelination defect persisted. These results further confirmed SC differentiation and myelin formation are separate events (Niemann et al., 2000; Novak et al., 2011), and that the myelination defect in shMLCK-treated cultures occurs at the post-transcriptional level.

Knockdown of MLCK impairs protein trafficking and results in increased lysosomal activity and protein degradation

Uncoupling of myelin assembly and SCs differentiation has been previously observed in transgenic rats overexpressing PMP22 (Niemann et al., 2000), and more recently in N-WASP-deficient mice (Novak et al., 2011). Similarly, in Trembler-J mutant mice defects in post-translational processing with increased protein degradation and lysosomal activity has been observed (Notterpek et al., 1997). To further characterize the nature of the myelination defect in cocultures established with SCs treated with shMLCK, we examine the activity of the lysosome-autophagosome pathway using antibodies to LAMP1 (Chen et al., 1985) and LC3B (Kabeya et al., 2000). In control cultures expression of both markers was progressively reduced as they myelinated (Fig. 7A). By contrast, we found that both LCB3 and LAMP1 expression remained higher in shMLCK-treated cultures (Fig. 7A), suggesting increased protein degradation in cultures that failed to myelinate. Normal myelin formation by SCs also requires protein sorting to different membrane domains along the endocytic and secretory pathways (Trapp et al., 1995; Yin et al., 2000). To assess whether protein trafficking was also impaired in shMLCK-treated cultures, we stained cultures with antibodies to transferrin receptor. We found that knockdown of MLCK resulted in prominent accumulation of transferrin receptor in the juxtanuclear Golgi region (Fig. 7B,C). This striking accumulation of vesicle-like structures was also observed in shMLCK-treated SC cultures and can be replicated by treatment of cultures with the MLCK inhibitor ML7 (supplementary material Movie 3). Taken together these data indicate that MLCK and myosin II activity are also required for protein trafficking in SCs and that in its absence abnormal protein accumulation and increased lysosomal activity might contribute to the myelination deficit observed in shMLCK-treated cultures.

Knockdown of MLCK impairs radial sorting of axons by Schwann cells

Electron microscopy analysis further confirmed the myelination in knockdown cultures (Fig. 8). Few axons were found to be myelinated in shMLCK-treated cultures, and among this population several abnormalities, such as thin myelin sheaths with compaction defects, were commonly observed (Fig. 8B; supplementary material Table S1). In addition SCs exhibiting a swollen rough endoplasmic reticulum (Fig. 8C) were frequently observed in shMLCK cultures (supplementary material Table S1), suggesting protein accumulation at this compartment. Although SCs in shMLCK cultures made contact with axons and produced a basal lamina, a significant proportion of them failed to fully segregate large caliber axons (greater than 1 μm diameter) in a 1:1 association (Fig. 8E,F) a precondition for normal SC myelination. We observed many examples of large and small caliber axons that were simultaneously surrounded by processes emanating from the same SCs or large axons that were incompletely segregated by a single SC (Fig. 8F). Of note, pronounced ensheathment defects were also observed in SCs lacking MLC (Wang et al., 2008), thus confirming that myosin II activity is required for proper axonal segregation. Thus, despite undergoing differentiation, shMLCK-treated SCs are unable to properly segregate axons and therefore unable to myelinate. Collectively, our data indicate that regulation of myosin II activity is required at different stages during myelination, including axonal sorting, activation of myelin gene transcription and myelin assembly (Fig. 9).

Discussion

In this study we analyzed the molecular events involved in cytoskeletal organization in SCs during in vitro differentiation and myelination. We have shown that the cytoskeletal changes

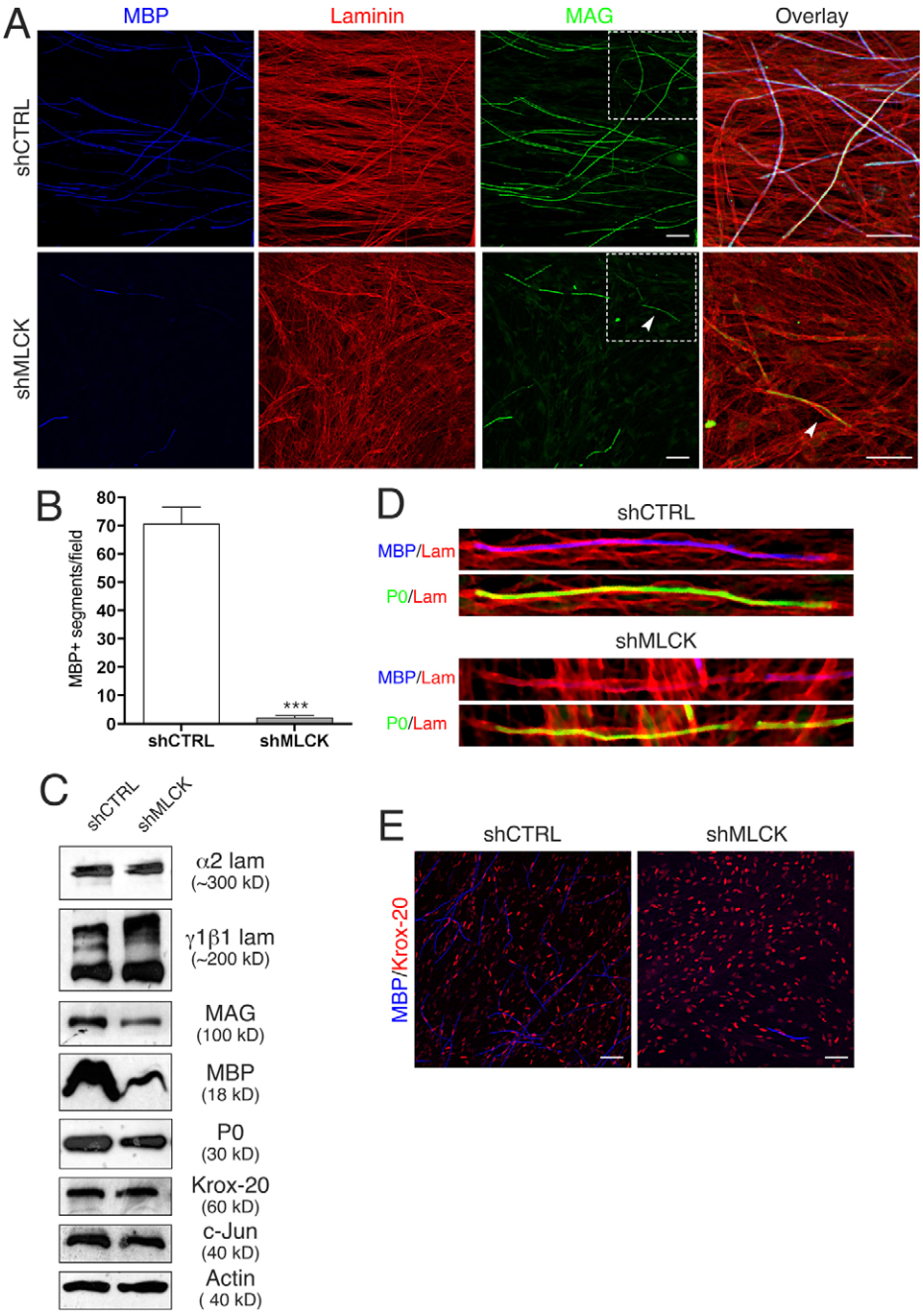

Fig. 5. Knockdown of MLCK in SCs inhibits myelination. (**A**) SCs infected with lentivirus constructs expressing non-targeting shRNA (shCTRL) or shRNA against MLCK (shMLCK) were seeded onto purified DRG neurons and allowed to myelinate for 18 days. Cultures were stained for MBP (blue), laminin (red) and MAG (green). A considerable reduction in the amount of MBP^+ segments is observed in cultures established with shMLCK SCs compared with controls. Despite the lack of MBP, staining for laminin shows the presence of basal lamina and in some cases expression of MAG. Scale bars: 50 μm. (**B**) Quantification of MBP^+ segments per field. Values are means ± s.e.m. of three independent experiments (three cultures per condition per experiment). (**C**) Western blots of myelinating cocultures showing a marked reduction on the levels of myelin proteins in shMLCK-treated cocultures. Levels of P0 and Krox-20 were reduced to a lesser extent whereas the expression of laminin chains was non-affected by shMLCK-treatment. (**D**) Detail of a myelinating coculture (14 days) showing an example of P0 expression (green) in the absence of MBP (blue) in shMLCK cultures. Basal lamina assembly (red) appears normal. (**E**) Myelinating cocultures (14 days) stained for Krox-20 and MBP. Despite the absence of myelin segments in shMLCK cultures Krox-20 upregulation can be detected in the nucleus of many MBP-negative SCs. Scale bars: 50 μm.

associated with the induction of the pro-myelinating program by cAMP in SCs, i.e. cell membrane expansion, stress fibers disassembly and downregulation of cytoskeletal contractility, are linked to decreased myosin II activity as shown by reduced MLC-*P* and MLCK levels (Fig. 2). Furthermore, knockdown of MLCK by shRNA reproduces the effects of cAMP-driven differentiation, stimulating cell-cycle arrest, downregulation of non-myelinating SCs markers and increased expression of pro-myelinating transcription factors and myelin proteins (Fig. 3A,B). Similarly, increased levels of MLC-*P* affect SC morphogenetic changes and their differentiation in response to cAMP (Fig. 3E,F). The localization of endogenous MLCK (Fig. 1) suggests that in addition to its role as a cytoskeletal regulator, MLCK might have an unknown role in the nucleus of SCs, a possibility that we are currently investigating.

Changes in MLC phosphorylation affect cytoskeleton plasticity and have been implicated in other cell differentiation processes including platelet development, lens fiber cell elongation and fibroblast decidualization (Chang et al., 2007; Chen et al., 2007; Ihnatovych et al., 2007; Maddala et al., 2007). Of note in vitro decidualization of human stromal fibroblasts, a process stimulated by cAMP elevation is also accompanied by downregulation of MLC phosphorylation (Ihnatovych et al., 2007). Phosphorylation inhibits the enzymatic activity of MLCK both in vitro and in vivo (Gallagher et al., 1997). MLCK can be phosphorylated by several kinases including PAK1 (Sanders

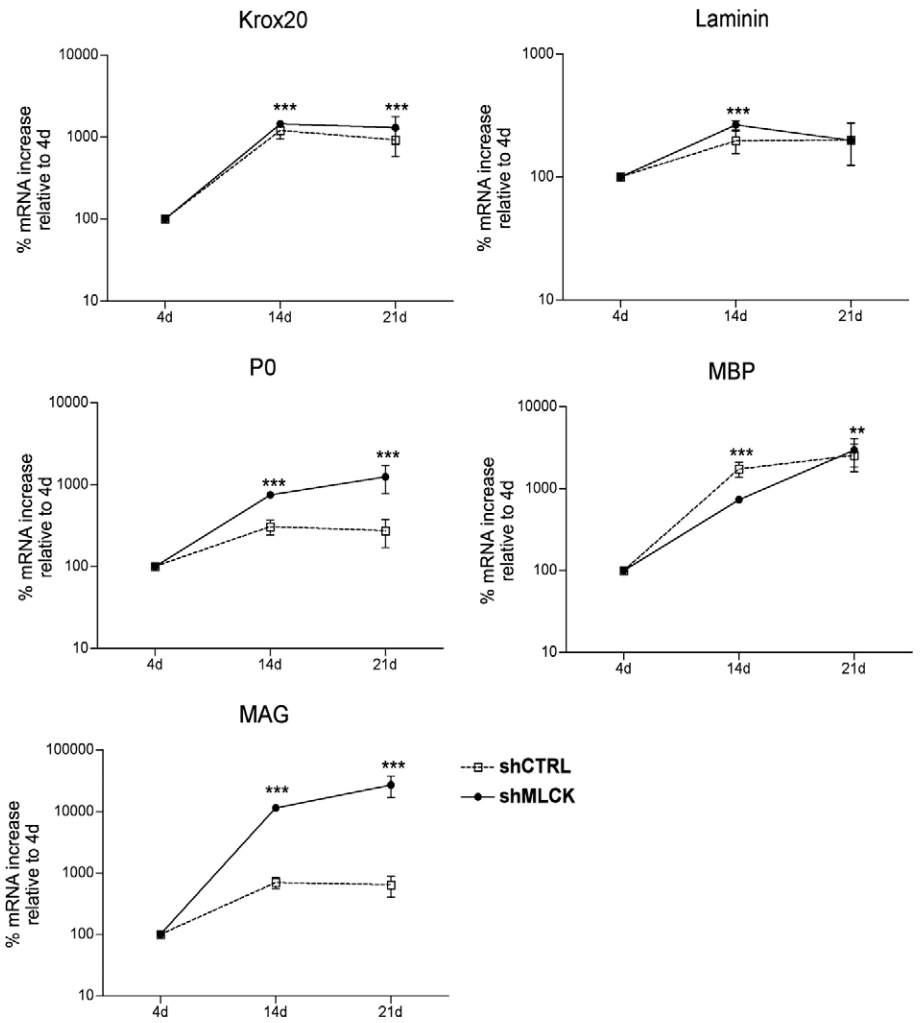

Fig. 6. Real-time PCR of myelinating cocultures. SCs infected with non-targeting shRNA (shCTRL) or shRNA against MLCK (shMLCK), were used to establish myelinating cocultures. RNA was isolated from a total of 12 cultures at the indicated time points and the relative increase of myelin protein mRNAs (P0, MBP and MAG), as well as Krox-20 and laminin mRNAs was measured by quantitative RT-PCR. Relative mRNA levels for each protein, normalized to actin (or L19), were calculated as indicated in Material and Methods. A significant increase in the relative amount of mRNA is observed for all proteins after 14 days (d) in coculture, reaching a plateau by 21 days. In shMLCK cultures (filled circles) the relative increase of mRNA is significantly higher (***$P<0.001$; **$P<0.01$, two-way ANOVA, Bonferroni post-test) than that of control cultures (open squares). The only exception was for the relative levels of MBP mRNA at 14 days, which was higher in control cultures.

et al., 1999) and PKA (de Lanerolle et al., 1984); and microinjection of activated PKA in fibroblasts or treatment with agents that elevate intracellular cAMP, result in marked alteration of cell morphology including disassembly of actin stress fibers (Lamb et al., 1988). Similar to our finding in SCs, these changes are also associated with an increase in MLCK phosphorylation and a decrease in MLC phosphorylation.

Collectively these data suggest that MLCK directly regulates actin cytoskeleton assembly and that an overall reduction of myosin-II-driven contraction following cAMP stimulation leads to dramatic morphological changes in SCs, including an increase in cell membrane expansion, a change that has been associated with activation of the myelination program (Morgan et al., 1991; Sobue and Pleasure, 1984). Of interest, a similar correlation between downregulation of acto-myosin contractility and membrane extension has been recently described during morphological differentiation of oligodendrocytes (Kippert et al., 2009), suggesting that despite their different morphologies and modes of myelination, the mechanisms controlling plasma membrane expansion by myelinating glial cells require local release of myosin-II-mediated contraction and relaxation of the actin cytoskeleton. Whether MLCK activity also plays a role in oligodendrocyte remodeling and differentiation awaits further study, but inactivation of RhoA and ROCK as well as inhibition of myosin II have been shown to promote membrane expansion and oligodendrocyte branching and differentiation (Kippert et al., 2007; Wang et al., 2008; Wolf et al., 2001).

Although, we did not detect changes in total levels of ROCK or MYPT1 after cAMP treatment (Fig. 2A), it is known that cAMP-dependent PKA can directly phosphorylate RhoA and promote its binding to the Rho dissociation inhibitor RhoGDI, sequestering Rho in its inactive GDP-bound form (reviewed by DerMardirossian and Bokoch, 2005). These data suggest that downregulation of RhoA activity, and, by extension, of its downstream target ROCK might also contribute to the initial reduction of MLC-*P* levels following cAMP. In agreement with this idea, we have found that upon treatment with cAMP the phophorylation of RhoA is increased in SCs (data not shown).

Our data also suggest that there is a reverse correlation between the levels of MLC-*P* and the SC differentiation. Thus, treatments that increase the basal levels of MLC-*P* (knockdown of MYPT1 or overexpression of constitutively active MLCK) resulted in decreased expression of differentiation markers (Fig. 3C), and reduced myelin formation in coculture (supplementary material Fig. S3). By contrast reduction of MLC-*P* levels by MLCK knockdown lead to increased myelination compared with control non-stimulated cultures (Fig. 3B). In agreement with these observations, we have also found that knockdown of total MLC

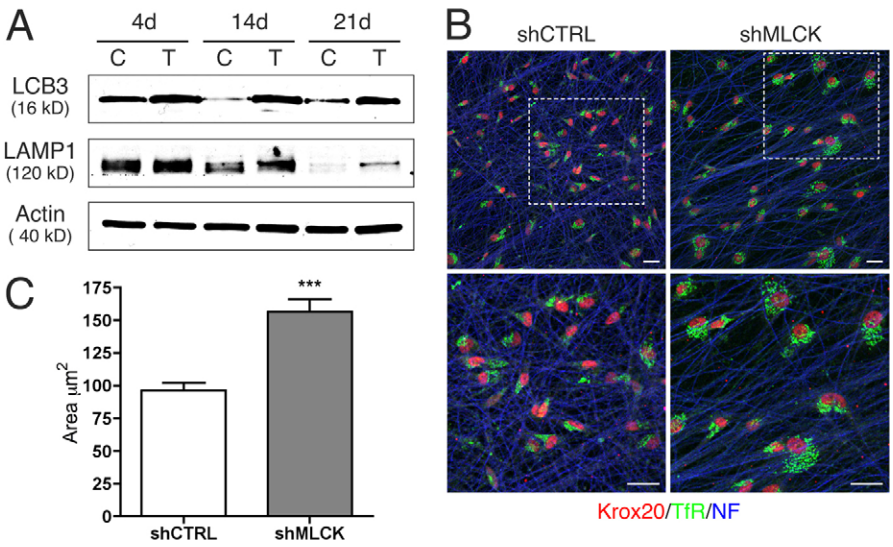

Fig. 7. Increased protein degradation and accumulation in MLCK-treated cocultures. (**A**) Lysates from shCTRL (C) and shMLCK-treated (T) cocultures were prepared at different days after the induction of myelination (4, 14 and 21 days; d) and probed with antibodies to LCB3 and LAMP1. The expression of both markers was increased in shMLCK cultures compared with controls. (**B**) SCs infected with lentivirus constructs expressing non-targeting shRNA (shCTRL) or shRNA against MLCK (shMLCK) were seeded onto purified DRG neurons and allowed to myelinate for 14 days. Cocultures were fixed and stained for Krox-20 (red), transferring receptor (green) and neurofilament (blue). Scale bars: 25 µm. (**C**) Quantification of transferrin staining area in cocultures. Values are means ± s.e.m. from two cultures. A total of 234 cells (128 shCTRL) and (106 shMLCK) were evaluated.

in SCs cultures alone results in increased MAG expression (supplementary material Fig. S2). We postulate that downregulation of MLC phosphorylation and myosin II activity is one of effects mediated by cAMP treatment that contributes to the changes in morphology and gene expression that accompany SCs differentiation (Monuki et al., 1989; Scherer et al., 1994). However this is not the only effect that downregulation of MLC activity has in SCs, as we have shown that ensheathment and sorting of axons (Wang et al., 2008) (Fig. 8), as well as the coordinate wrapping of SCs around them (Melendez-Vasquez et al., 2004) requires MLC activity. Thus we proposed that myosin II activity in SCs might play different roles at different stages of SCs differentiation (Fig. 9).

In agreement with this interpretation, we found that despite activation of myelin gene transcription, when placed in contact with axons SCs lacking MLCK fail to myelinate, thus uncoupling the process of SCs differentiation from compact myelin assembly. Although, this result appears counterintuitive, dissociation of SCs differentiation from myelin formation has been previously reported in hypomyelinating animal models such as transgenic rats overexpressing PMP22 (Niemann et al., 2000), and more recently in N-WASP conditional knockout mice (Novak et al., 2011). Similarly in the CNS, uncoupling of oligodendrocyte differentiation as evidenced by MBP expression and myelination has been extensively documented (for a review, see Rosenberg et al., 2007).

Although cAMP can mimic some aspects of SC–axon interaction, it certainly does not recapitulate the full complexity of signaling between these cells. It is well known that SC responses to axon-derived signals such as neuregulin depend on whether the signal is presented in a paracrine or juxtacrine context (Syed et al., 2010; Zanazzi et al., 2001). Similarly, although Erk activation appears to be necessary for dedifferentiation of SCs in coculture with axons, it is not required for dedifferentiation of purified SCs (Monje et al., 2010). There is also a lack of spatial polarization in SC cultures when compared with the establishment of abaxonal and adaxonal surfaces of SCs in contact with axons.

We propose that the effects on SC cytoskeleton and gene transcription observed after MLCK knockdown are controlled in a temporal and spatially restricted manner by the axon. Thus, activation of adenyl cyclase and elevation of intracellular cAMP levels after contact between the adaxonal SC membrane and the axolemma, might promote local downregulation of MLCK and myosin II contractility, leading to the initial extension and wrapping of the inner mesaxon, a process that might be powered by actin polymerization at the cell cortex. This mechanism is akin to that described for the extension of lamellipodia at the leading edge of motile cells (Chhabra and Higgs, 2007). However, further radial growth of the myelin sheath requires coordination between the ‘wrapping’ motor and the delivery and incorporation of myelin proteins at the membrane. Our data suggest that MLCK might also be involved in protein trafficking (see below). Therefore a local balance between the extent of myosin II activity and actin polymerization is necessary to establish normal SC myelination.

Downregulation of MLCK levels in SCs results in a substantial reduction of MBP mRNA and protein expression in SC–neuronal cocultures. MBP mRNA is transported from the nucleus towards the plasma membrane in RNA–protein complexes, which are locally translated at the sites of compact myelin assembly (Colman et al., 1982; Gould and Mattingly, 1990). Thus it is possible that defective transport of MBP mRNA contributes to the myelination deficit observed in shMLCK cultures. Of note, targeting of actin mRNA to the plasma membrane has been shown to depend on acto-myosin II motors, which in turn are regulated by MLCK (Latham et al., 2001). Despite reduced protein levels, expression of Krox-20, P0 and MAG mRNA were actually increased in shMLCK cultures, possibly as a

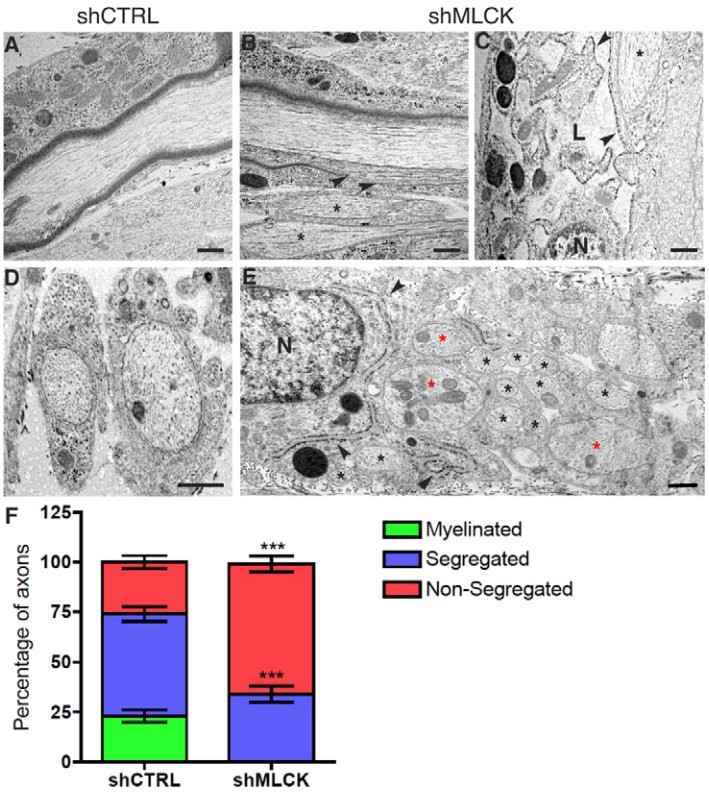

Fig. 8. Ultrastructural analysis of myelinating cocultures. (**A**) Longitudinal section of a myelinated axon in an 18-day-old control coculture. (**B**) Unevenly myelinated axon in an18-day-old shMLCK culture. Arrowheads indicate aberrant compaction on one side of the internode. Asterisks mark two unmyelinated axons. (**C**) Detail of an abnormally enlarged rough endoplasmic reticulum (rER) in a non-myelinating shMLCK SC. The swollen and prominent lumen (L) of the rER and attached ribosomes (arrowheads) are visible. N denotes the nucleus of the SC. A non-myelinated axon (asterisk) is indicated. (**D**) Cross section of two axons segregated in a 1:1 association in control cultures. (**E**) Example of incomplete sorting by SCs in shMLCK cultures. Many small (black asterisks) and large (red asterisks) caliber axons are contained within the cytoplasm of this cell and are not properly segregated. Prominent ER (arrowheads) and SC nucleus (N) are also visible. Scale bars: 500 nm. (**F**) Percentage of myelinated, segregated or non-segregated axons in shCTRL and shMLCK cultures. Values are means ± s.e.m. from four cultures (two per condition). A total of 645 axons were counted (318 from shCTRL; 327 from shMLCK).

compensatory mechanism. These observations suggest that the blockade of myelination in these cultures reflects a post-transcriptional defect. The prominent localization of MLCK in the perinuclear region of SCs (Fig. 1), as well as the accumulation of transferring receptor, increased lysosomal activity (Fig. 7), and the presence of swollen ER in shMLCK-treated SCs (Fig. 8) suggests abnormal protein trafficking. In potential agreement with this idea, a more direct role for MLCK and myosin-II-based motors in vesicle production and transport (DePina et al., 2007; Musch et al., 1997), as well as in endocytic and exocytic events (Andzelm et al., 2007; Marchiando et al., 2010; Togo and Steinhardt, 2004), has also been described.

We also found that MLCK is highly expressed in the SC nucleus both in vivo and in vitro, as well as in optic nerve oligodendrocytes at the onset of myelination (M.U. and C.V.M.-V., unpublished data). Although reports of the expression of MLCK in non-muscle cells using GFP-tagged constructs have described its localization in the cytoplasm and certain actin-rich structures such as stress fibers and membrane ruffles (Blue et al., 2002; Poperechnaya et al., 2000), there are also several reports

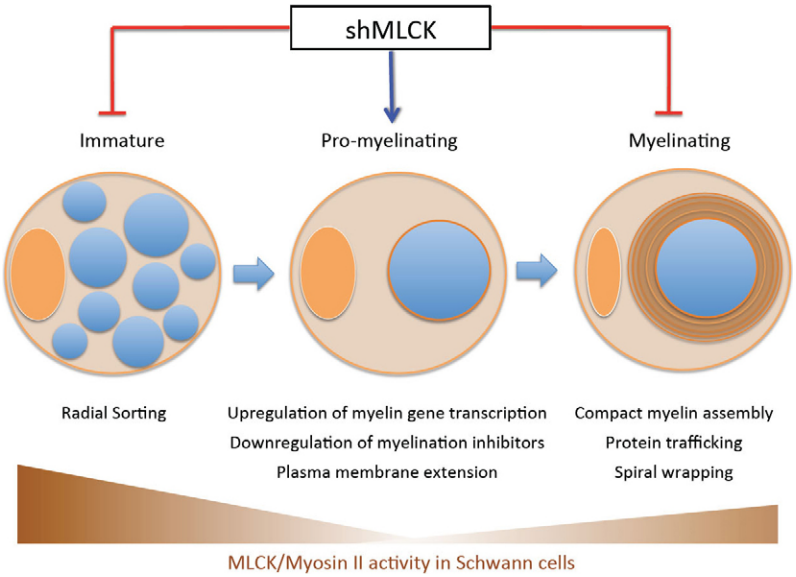

Fig. 9. A model of changes in non-muscle myosin II activity during SC development. In immature SCs, the activity of myosin II is higher than in mature differentiated cells (Melendez-Vasquez et al., 2004; Wang et al., 2008). Myosin II activity is required for radial sorting of axons and this process is impaired by knockdown of shMLCK (Wang et al., 2008) (this study). Once the SC has achieved a 1:1 association with the axon (pro-myelinating stage), the activation of myelin gene transcription and membrane expansion is correlated with a marked downregulation of myosin II activity, a process that can be recapitulated in SCs cultures by knockdown of MLCK and/or treatment with cAMP (this study). Later morphogenetic events, such as the wrapping of compact myelin around the axons, requires coordination between the synthesis of myelin proteins and their trafficking to the plasma membrane, processes in which myosin II and MLCK also appear to play a role (Melendez-Vasquez et al., 2004) (this study). Orange ovals, SC nuclei; blue circles, axons; red lines, inhibition; blue arrow, activation.

describing the presence of its endogenous targets (myosin II and/or MLC) in the nucleus of human and rodent cells (Li and Sarna, 2009; Ray et al., 2007). MLCK activity has been shown to be necessary for TNFα-dependent NFκB activation and amplification of pro-survival signals (Wadgaonkar et al., 2003). Although a role for nuclear actin and myosin I motors during transcription has been established (Hofmann et al., 2004; Philimonenko et al., 2004), it is unclear whether this model extends to other myosin motors (Li and Sarna, 2009).

Finally, we cannot rule out that in addition to our interpretation of spatial and temporal regulation of MLC phosphorylation, additional targets for MLCK exist in SCs. Myosin-II-independent function has been described during neutrophil transmigration where MLCK is required for the activation of tyrosine kinase Pyk2 (Xu et al., 2008). Although we found that SCs express Pyk2, its total levels and phosphorylation status where not altered by cAMP treatment or after MLCK knockdown (data not shown).

In conclusion, our study provides novel evidence supporting an important role for MLCK as a regulator of SC differentiation and myelination. Local changes in the SC cytoskeleton plasticity and organization are in turn important to establish proper axonal sorting, myelin protein expression and transport (Fig. 9). The elucidation of the temporal and spatial regulation of myosin II activity and actin polymerization in SCs will contribute to a better understanding of the mechanistic complexity of myelination.

Materials and Methods

Schwann cell cultures

SCs were isolated from postnatal day 2 rat sciatic nerves and expanded for 3 weeks in M medium (minimum essential medium, 10% FBS and 2 mM L-glutamine) supplemented with 4 μM forskolin (Sigma) and 5 ng/ml of the EGF domain of recombinant human neuregulin-1-β1 (rhNRG-1-β1; R&D Systems), which is called M^+ medium. For studies on the effects of cAMP analogues on SC differentiation, cultures maintained in M^+ medium were switched to medium without growth factors for 3 days (M medium). SCs were either starved overnight in serum-free M medium (MEM and 2 mM L-glutamine) or placed in defined medium DM (DMEM–F12, 5 μg/ml insulin, 5 μg/ml transferrin) prior to treatment with 1 mM dibutyryl cyclic adenosine monophosphate (db-cAMP; Calbiochem) for 30 minutes, 24 hours, 48 hours and 72 hours. At the indicated time points, cells were lysed and subjected to SDS-PAGE as described below. For immunocytochemistry, SCs were plated on poly-L-lysine-coated glass coverslips at a density of 20,000 cells per coverslip, treated with db-cAMP as described and processed for immunofluorescence.

Myelinating cocultures

DRG neurons were isolated from embryonic day 16 rat spinal cords and either trypsinized or directly plated as explants on collagen-coated coverslips (BD Biosciences). Cultures were maintained in serum-free neurobasal medium (NB medium: 2% B27 supplement, 2 mM L-glutamine, 0.4% glucose and 50 ng/ml 2.5S nerve growth factor; NGF). Nonneuronal cells were removed by feeding the cultures with NB medium containing 5-fluorodeoxyuridine and uridine. Myelinating cocultures were established by seeding purified DRG neuron cultures with 100,000 SCs in C medium (MEM, 10% FBS, 2 mM L-glutamine, 0.4% glucose and 50 ng/ml 2.5S NGF). After 3 days, cocultures were changed to medium supplemented with 50 μg/ml ascorbic acid to initiate basal lamina formation and myelination. For studies of the effects of MLCK inhibition on myelination, cocultures were switched to myelin-promoting medium containing ML7 (EMD Chemicals). Control and treated cultures were allowed to myelinate for 2–3 weeks, with fresh medium provided every 2–3 days. To determine the extent of myelination in SC–DRG cocultures, the total numbers of MBP^+ segments were counted in micrographs from 10–12 random low-power (20×) fields per coverslip using ImageJ, version 1.38 (total of 20–24 fields per condition per experiment; total of two to three experiments). Statistical tests (*t*-test and ANOVA) were performed using GraphPad Prism (GraphPad Software).

shRNA of MLCK in SCs and myelinating cocultures

The LKO.1 lentiviral vectors expressing shRNA against MLCK and MYPT1 were obtained from Sigma-Aldrich (Mission® shRNA). The shRNA oligo sequences used in this study were: MLCK, 5′-GCTAGATTTGACTGCAAGATT-3′ (TRCN0000024034), 5′-ACTGTCCTCTATGGCAATGAT-3′ (TRCN0000000936); and MYPT1 5′-GCCTTTGATGTAGCAGATGAA-3′ (TRCN 0000002445); 5′-TCTCGTCCTCTTTGGATAATA-3′ (TRCN0000240624). LKO.1 plasmids were cotransfected along with Δ8.9 and pCMV-VSVG plasmids into 293FT cells utilizing Lipofectamine 2000 (Invitrogen). As control (shCTRL), we used a non-targeting vector (SHC002). Viral supernatants were collected 72 hours after transfection, centrifuged at 1000 ***g*** for 15 minutes, aliquoted for one-time use, and frozen at −80℃. Freshly plated SCs were incubated for 5 days with viruses at a 2:3 dilution (vol/vol) in M^+ medium. Cells were then trypsinized and seeded onto DRG neurons for myelination experiments or seeded onto PLL- or PLL–laminin-coated coverslips for SC-only experiments. Protein knockdown was confirmed by western blotting. For estimation of knockdown efficiency, X-ray films from two to three independent experiments were scanned and the relative intensity of each protein band was calculated in Adobe Photoshop by dividing the absolute intensity of each protein band (the area of the band multiplied by the number of pixels contained in that area) by the absolute intensity of the corresponding actin band.

Electron microscopy

shCTRL- and shMLCK-treated myelinating cocultures were rinsed in PBS, fixed overnight at 4℃ in 2% glutaraldehyde in 0.1 M phosphate buffer, pH 7.0, and processed further as described previously (Einheber et al., 1995). Specimens were examined on a Philips (Eindhoven, The Netherlands) CM10 electron microscope.

Proliferation assays

To investigate the effect of MLCK inhibition on the proliferation of SCs, bromodeoxyuridine (BrdU) incorporation assays were performed as described previously (Wang et al., 2008). Briefly, SCs were infected with shCTRL and shMLCK lentiviral supernatant for 5 days, after which 15,000 SCs were plated onto PLL-coated glass coverslips and maintained for 24 hours in medium with forskolin and 5 ng/ml of the EGF domain of rhNRG-1-β1. We also examined SCs proliferating in cocultures with DRG neurons. For these studies, 50,000 SCs in C medium (MEM, 10% FBS, 2 mM L-glutamine, 0.4% glucose and 50 ng/ml 2.5S NGF) were seeded onto dissociated DRG neurons. After 48 hours, cultures were then processed for BrdU immunostaining. In all conditions, BrdU was added during the last 4 hours of culture at a final concentration of 20 μM; immunostaining was performed according to the instructions of the manufacturer (Boehringer Mannheim).

Antibodies

Antibodies used in these studies included those reactive to: MBP (SMI-94) and neurofilament (SMI-31 and SMI-32; Sternberger Monoclonals); MLC2, phosphorylated MLC2, MYPT1 and LC3B (Cell Signaling Technology); phalloidin–FITC, phalloidin–TRITC, phalloidin–coumarin, rabbit EHS laminin and actin (Sigma-Aldrich); phosphorylated MLCK (Invitrogen); GFP (Millipore); p27 (C-19; Santa Cruz Biotechnology, Inc.); c-Jun and N-cadherin (BD Biosciences); LAMP1 (Abcam) and transferrin receptor (Zymed). Polyclonal antibodies to Krox-20 and Oct-6 (provided by Dies Meijer, Erasmus University, Rotterdam, Netherlands), MAG (Pedraza et al., 1990), P0 (Marie Filbin, Hunter College, City University of New York, New York, NY), laminin a-2 chain (Peter Yurchenco, Robert Wood Johnson Medical School, University of Medicine and Dentistry of New Jersey, Piscataway, NJ); affinity purified rabbit and goat anti-MLCK (de Lanerolle et al., 1981; de Lanerolle et al., 1987) were also used. Secondary antibodies conjugated to Rhodamine, fluorescein, coumarin or cyanin 5 were obtained from Jackson ImmunoResearch Laboratories.

Immunofluorescence

Cultures (SCs and myelinating co-cultures) were fixed in 4% PFA containing 5% sucrose, permeabilized with 0.5% Triton X-100 and processed for immunocytochemistry as described previously (Wang et al., 2008). Cultures were examined by epifluorescence or confocal microscopy.

Image acquisition and analysis

Epifluorescence images were acquired using a Leica DMI 4000B microscope (LAS 1.7.0 software) equipped with a Leica DFC350FX digital camera and the following Leica objectives: N PLAN 10×, 0.25 NA; N PLAN L 40×, 0.55 NA and HCX PL APO CS 63×, 1.4 NA oil UV. Confocal images were acquired with a Zeiss LSM 510 using Plan-Apochromat 20×, 0.75 NA or Neofluor 40×, 1.3 NA oil Zeiss objectives and LSM software. Image processing and quantification were performed using ImageJ (v1.38) and Adobe Photoshop CS8. Adjustment of image brightness or contrast was performed in some cases but without misrepresenting data.

Time-lapse microscopy

Movies were acquired with a Leica DMI4000B microscope system fitted with a stage incubator and a temperature and CO_2 digital controller (CTI Controller 37000, Pecon), or with a Vivaview FL incubator fluorescence microscope (Olympus). Cells were plated on PLL-coated glass-bottomed 35-mm tissue culture

dishes (MatTek). Images were acquired using a N PLAN L 40×, 0.55 NA or HCX PL APO CS 63×, 1.4 NA oil UV objectives (Leica microscope) or UPLSAPO 20×, 0.75 NA (Olympus microscope). Cultures were maintained at 37℃ and 5% CO_2 throughout the observation period.

Subcellular fractionation

Schwann cells maintained on PLL-coated 10 cm plastic dishes in M^+ medium were briefly washed with ice-cold PBS, collected by centrifugation at 4℃ at 400 ***g*** and subjected to subcellular fractionation using a ProteoExtract subcellular proteome extraction kit (Calbiochem) according to the manufacturer's protocol. Fractions were analyzed by western blotting (4% of each fraction) as described below.

Cell extracts and western blotting

Schwann cells and myelinating cocultures were lysed in a solution containing 2% SDS, 150 mM NaCl, 10 mM EDTA, 1 mM PMSF, 10 µg/ml aprotinin and 20 µM leupeptin in 50 mM Tris, pH 7.4. Lysates were cleared by centrifugation at 10,000 ***g*** for 10 minutes. Protein concentrations were determined using the BCA method (Pierce). Lysates (10–30 µg of total protein) were subjected to SDS-PAGE and blotted onto nitrocellulose. Appropriate regions of the blots were cut out, incubated with specific antibodies and developed using the West Pico chemiluminescent substrate (Pierce).

Real-time PCR

RNA was harvested using an Absolutely-RNA RT-PCR Miniprep kit (Stratagene). cDNA was generated, and real-time PCR performed, using a previously published protocol (Yuen et al., 2002b). Each transcript in each sample was assayed in triplicate, and the mean detection threshold (*Ct*) values were used to calculate fold-change ratios between experimental and control samples for each gene. Amplicon size and reaction specificity were confirmed by agarose gel electrophoresis. Data validity by modeling of reaction efficiency and analysis of measurement precision has been described previously (Yuen et al., 2002a). The primers used included: actin, sense 5′-AGCCATGTACGTAGCCATCC-3′, antisense 5′-CTCTCAGCTGTGGTGGTGAA-3′; product, 228 bp; L19, sense 5′-CATGGAGCACATCCACAAAC-3′, antisense 5′-CCATAGCCTGGCCACTATGT-3′; product, 216 bp; Krox-20, sense 5′-CATCTCTGCGCCTAGAAACC-3′, antisense 5′-GAAGAGGCTGTGGTTGAAGC-3′; product, 159 bp; laminin, sense 5′-CACAGTGGGGTCCTTGTCTT-3′, antisense 5′-AGTGGACACCTTCCACGTTC-3′; product, 245 bp; MAG, sense 5′-GAAACTGCACCCTGCTTCTC-3′, antisense 5′-CACCATGCAGCTGACCTCTA-3′; product size, 191 bp; P0, sense 5′-CTTCCAAAGGCTCTCAGGTG-3′, antisense 5′-ACGGTCACTTGTTCGAGTCC-3′; product size, 153 bp; MBP, sense 5′-ACACAAGAACTACCCACTACGG-3′, antisense 5′-GGGTGTACGAGGTGTCACAA-3′; product size, 110 bp. Relative mRNA levels for each protein normalized to actin (or L19), were calculated as follows: $1.93^{[\Delta Ct(shCTRL)-\Delta Ct(shMLCK)]}=1.93^{\Delta Ct}$, where ΔCt equals Ct(actin)–Ct(protein) calculated for each culture condition at each time point (Zalfa et al., 2007). Statistical analysis (two-way ANOVA or Bonferroni post-test) was performed using GraphPad Prism (GraphPad Software).

Acknowledgements

We thank Charlotte D'Hulst for helping with quantitative RT-PCR data analyses; Ananya Sengupta for assistance with electron microscopy quantification, Teresa Milner for her help with electron microscopy studies, and Carla Taveggia, Robert Fischer, Haesun Kim, Patrice Maurel and Gareth John, for helpful discussion about the manuscript.

Funding

This study was supported by National Institutes of Health [grant numbers NS052259 to C.M.-V., GM80587 to P.de L.]; and a core facility grant from the National Center for Research Resources [grant number RR03037]. Deposited in PMC for release after 12 months.

Supplementary material available online at
http://jcs.biologists.org/lookup/suppl/doi:10.1242/jcs.080200/-/DC1

References

Adelstein, R. S. and Conti, M. A. (1975). Phosphorylation of platelet myosin increases actin activated myosin ATPase activity. *Nature* **256**, 597-598.

Andzelm, M. M., Chen, X., Krzewski, K., Orange, J. S. and Strominger, J. L. (2007). Myosin IIA is required for cytolytic granule exocytosis in human NK cells. *J. Exp. Med.* **204**, 2285-2291.

Benninger, Y., Thurnherr, T., Pereira, J. A., Krause, S., Wu, X., Chrostek-Grashoff, A., Herzog, D., Nave, K. A., Franklin, R. J., Meijer, D. et al. (2007). Essential and distinct roles for cdc42 and rac1 in the regulation of Schwann cell biology during peripheral nervous system development. *J. Cell Biol.* **177**, 1051-1061.

Blue, E. K., Goeckeler, Z. M., Jin, Y., Hou, L., Dixon, S. A., Herring, B. P., Wysolmerski, R. B. and Gallagher, P. J. (2002). 220- and 130-kDa MLCKs have distinct tissue distributions and intracellular localization patterns. *Am. J. Physiol. Cell Physiol.* **282**, C451-C460.

Bunge, R. P., Bunge, M. B. and Bates, M. (1989). Movements of the Schwann cell nucleus implicate progression of the inner (axon-related) Schwann cell process during myelination. *J. Cell Biol.* **109**, 273-284.

Chang, Y., Aurade, F., Larbret, F., Zhang, Y., Le Couedic, J. P., Momeux, L., Larghero, J., Bertoglio, J., Louache, F., Cramer, E. et al. (2007). Proplatelet formation is regulated by the Rho/ROCK pathway. *Blood* **109**, 4229-4236.

Chen, J. W., Murphy, T. L., Willingham, M. C., Pastan, I. and August, J. T. (1985). Identification of two lysosomal membrane glycoproteins. *J. Cell Biol.* **101**, 85-95.

Chen, Z., Naveiras, O., Balduini, A., Mammoto, A., Conti, M. A., Adelstein, R. S., Ingber, D., Daley, G. Q. and Shivdasani, R. A. (2007). The May-Hegglin anomaly gene MYH9 is a negative regulator of platelet biogenesis modulated by the Rho-ROCK pathway. *Blood* **110**, 171-179.

Chhabra, E. S. and Higgs, H. N. (2007). The many faces of actin: matching assembly factors with cellular structures. *Nat. Cell Biol.* **9**, 1110-1121.

Colman, D. R., Kreibich, G., Frey, A. B. and Sabatini, D. D. (1982). Synthesis and incorporation of myelin polypeptides into CNS myelin. *J. Cell Biol.* **95**, 598-608.

de Lanerolle, P., Adelstein, R. S., Feramisco, J. R. and Burridge, K. (1981). Characterization of antibodies to smooth muscle myosin kinase and their use in localizing myosin kinase in nonmuscle cells. *Proc. Natl. Acad. Sci. USA* **78**, 4738-4742.

de Lanerolle, P., Nishikawa, M., Yost, D. A. and Adelstein, R. S. (1984). Increased phosphorylation of myosin light chain kinase after an increase in cyclic AMP in intact smooth muscle. *Science* **223**, 1415-1417.

de Lanerolle, P., Nishikawa, M., Felsen, R. and Adelstein, R. S. (1987). Immunological properties of myosin light-chain kinases. *Biochim. Biophys. Acta* **914**, 74-82.

DePina, A. S., Wollert, T. and Langford, G. M. (2007). Membrane associated nonmuscle myosin II functions as a motor for actin-based vesicle transport in clam oocyte extracts. *Cell Motil. Cytoskeleton* **64**, 739-755.

DerMardirossian, C. and Bokoch, G. M. (2005). GDIs: central regulatory molecules in Rho GTPase activation. *Trends Cell Biol.* **15**, 356-363.

Einheber, S., Hannocks, M. J., Metz, C. N., Rifkin, D. B. and Salzer, J. L. (1995). Transforming growth factor-beta 1 regulates axon/Schwann cell interactions. *J. Cell Biol.* **129**, 443-458.

Gallagher, P. J., Herring, B. P. and Stull, J. T. (1997). Myosin light chain kinases. *J. Muscle Res. Cell Motil.* **18**, 1-16.

Gould, R. M. and Mattingly, G. (1990). Regional localization of RNA and protein metabolism in Schwann cells in vivo. *J. Neurocytol.* **19**, 285-301.

Hofmann, W. A., Stojiljkovic, L., Fuchsova, B., Vargas, G. M., Mavrommatis, E., Philimonenko, V., Kysela, K., Goodrich, J. A., Lessard, J. L., Hope, T. J. et al. (2004). Actin is part of pre-initiation complexes and is necessary for transcription by RNA polymerase II. *Nat. Cell Biol.* **6**, 1094-1101.

Ihnatovych, I., Hu, W., Martin, J. L., Fazleabas, A. T., de Lanerolle, P. and Strakova, Z. (2007). Increased phosphorylation of myosin light chain prevents in vitro decidualization. *Endocrinology* **148**, 3176-3184.

Kabeya, Y., Mizushima, N., Ueno, T., Yamamoto, A., Kirisako, T., Noda, T., Kominami, E., Ohsumi, Y. and Yoshimori, T. (2000). LC3, a mammalian homologue of yeast Apg8p, is localized in autophagosome membranes after processing. *EMBO J.* **19**, 5720-5728.

Kimura, K., Ito, M., Amano, M., Chihara, K., Fukata, Y., Nakafuku, M., Yamamori, B., Feng, J., Nakano, T., Okawa, K. et al. (1996). Regulation of myosin phosphatase by Rho and Rho-associated kinase (Rho-kinase). *Science* **273**, 245-248.

Kippert, A., Trajkovic, K., Rajendran, L., Ries, J. and Simons, M. (2007). Rho regulates membrane transport in the endocytic pathway to control plasma membrane specialization in oligodendroglial cells. *J. Neurosci.* **27**, 3560-3570.

Kippert, A., Fitzner, D., Helenius, J. and Simons, M. (2009). Actomyosin contractility controls cell surface area of oligodendrocytes. *BMC Cell Biol.* **10**, 71.

Lamb, N. J., Fernandez, A., Conti, M. A., Adelstein, R., Glass, D. B., Welch, W. J. and Feramisco, J. R. (1988). Regulation of actin microfilament integrity in living nonmuscle cells by the cAMP-dependent protein kinase and the myosin light chain kinase. *J. Cell Biol.* **106**, 1955-1971.

Larocque, D., Fragoso, G., Huang, J., Mushynski, W. E., Loignon, M., Richard, S. and Almazan, G. (2009). The QKI-6 and QKI-7 RNA binding proteins block proliferation and promote Schwann cell myelination. *PLoS One* **4**, e5867.

Latham, V. M., Yu, E. H., Tullio, A. N., Adelstein, R. S. and Singer, R. H. (2001). A Rhodependent signaling pathway operating through myosin localizes beta-actin mRNA in fibroblasts. *Curr. Biol.* **11**, 1010-1016.

Li, Q. and Sarna, S. K. (2009). Nuclear myosin II regulates the assembly of preinitiation complex for ICAM-1 gene transcription. *Gastroenterology* **137**, 1051-1060.

Maddala, R., Skiba, N. and Vasantha Rao, P. (2007). Lens fiber cell elongation and differentiation is associated with a robust increase in myosin light chain phosphorylation in the developing mouse. *Differentiation* **75**, 713-725.

Marchiando, A. M., Shen, L., Graham, W. V., Weber, C. R., Schwarz, B. T., Austin, J. R., 2nd, Raleigh, D. R., Guan, Y., Watson, A. J., Montrose, M. H. et al. (2010).

Caveolin-1-dependent occluding endocytosis is required for TNF-induced tight junction regulation in vivo. *J. Cell Biol.* **189**, 111-126.

Melendez-Vasquez, C. V., Einheber, S. and Salzer, J. L. (2004). Rho kinase regulates Schwann cell myelination and formation of associated axonal domains. *J. Neurosci.* **24**, 3953-3963.

Michailov, G. V., Sereda, M. W., Brinkmann, B. G., Fischer, T. M., Haug, B., Birchmeier, C., Role, L., Lai, C., Schwab, M. H. and Nave, K. A. (2004). Axonal neuregulin-1 regulates myelin sheath thickness. *Science* **304**, 700-703.

Monje, P. V., Rendon, S., Athauda, G., Bates, M., Wood, P. M. and Bunge, M. B. (2009). Nonantagonistic relationship between mitogenic factors and cAMP in adult Schwann cell re-differentiation. *Glia* **57**, 947-961.

Monje, P. V., Soto, J., Bacallao, K. and Wood, P. M. (2010). Schwann cell dedifferentiation is independent of mitogenic signaling and uncoupled to proliferation: role of cAMP and JNK in the maintenance of the differentiated state. *J. Biol. Chem.* **285**, 31024-31036.

Monk, K. R., Naylor, S. G., Glenn, T. D., Mercurio, S., Perlin, J. R., Dominguez, C., Moens, C. B. and Talbot, W. S. (2009). A G protein-coupled receptor is essential for Schwann cells to initiate myelination. *Science* **325**, 1402-1405.

Monuki, E. S., Weinmaster, G., Kuhn, R. and Lemke, G. (1989). SCIP: a glial POU domain gene regulated by cyclic AMP. *Neuron* **3**, 783-793.

Morgan, L., Jessen, K. R. and Mirsky, R. (1991). The effects of cAMP on differentiation of cultured Schwann cells: progression from an early phenotype (04+) to a myelin phenotype (P0+, GFAP-, NCAM-, NGF-receptor-) depends on growth inhibition. *J. Cell Biol.* **112**, 457-467.

Musch, A., Cohen, D. and Rodriguez-Boulan, E. (1997). Myosin II is involved in the production of constitutive transport vesicles from the TGN. *J. Cell Biol.* **138**, 291-306.

Niemann, S., Sereda, M. W., Suter, U., Griffiths, I. R. and Nave, K. A. (2000). Uncoupling of myelin assembly and Schwann cell differentiation by transgenic overexpression of peripheral myelin protein 22. *J. Neurosci.* **20**, 4120-4128.

Nodari, A., Zambroni, D., Quattrini, A., Court, F. A., D'Urso, A., Recchia, A., Tybulewicz, V. L., Wrabetz, L. and Feltri, M. L. (2007). Beta1 integrin activates Rac1 in Schwann cells to generate radial lamellae during axonal sorting and myelination. *J. Cell Biol.* **177**, 1063-1075.

Notterpek, L., Shooter, E. M. and Snipes, G. J. (1997). Upregulation of the endosomal-lysosomal pathway in the trembler-J neuropathy. *J. Neurosci.* **17**, 4190-4200.

Novak, N., Bar, V., Sabanay, H., Frechter, S., Jaegle, M., Snapper, S. B., Meijer, D. and Peles, E. (2011). N-WASP is required for membrane wrapping and myelination by Schwann cells. *J. Cell Biol.* **192**, 243-250.

Parkinson, D. B., Bhaskaran, A., Droggiti, A., Dickinson, S., D'Antonio, M., Mirsky, R. and Jessen, K. R. (2004). Krox-20 inhibits Jun-NH2-terminal kinase/c-Jun to control Schwann cell proliferation and death. *J. Cell Biol.* **164**, 385-394.

Parkinson, D. B., Bhaskaran, A., Arthur-Farraj, P., Noon, L. A., Woodhoo, A., Lloyd, A. C., Feltri, M. L., Wrabetz, L., Behrens, A., Mirsky, R. et al. (2008). c-Jun is a negative regulator of myelination. *J. Cell Biol.* **181**, 625-637.

Pedraza, L., Owens, G. C., Green, L. A. and Salzer, J. L. (1990). The myelin-associated glycoproteins: membrane disposition, evidence of a novel disulfide linkage between immunoglobulin-like domains, and posttranslational palmitylation. *J. Cell Biol.* **111**, 2651-2661.

Pereira, J. A., Benninger, Y., Baumann, R., Goncalves, A. F., Ozcelik, M., Thurnherr, T., Tricaud, N., Meijer, D., Fassler, R., Suter, U. et al. (2009). Integrin-linked kinase is required for radial sorting of axons and Schwann cell remyelination in the peripheral nervous system. *J. Cell Biol.* **185**, 147-161.

Philimonenko, V. V., Zhao, J., Iben, S., Dingova, H., Kysela, K., Kahle, M., Zentgraf, H., Hofmann, W. A., de Lanerolle, P., Hozak, P. et al. (2004). Nuclear actin and myosin I are required for RNA polymerase I transcription. *Nat. Cell Biol.* **6**, 1165-1172.

Poperechnaya, A., Varlamova, O., Lin, P. J., Stull, J. T. and Bresnick, A. R. (2000). Localization and activity of myosin light chain kinase isoforms during the cell cycle. *J. Cell Biol.* **151**, 697-708.

Ray, R. M., Guo, H., Patel, M., Jin, S., Bhattacharya, S. and Johnson, L. R. (2007). Role of myosin regulatory light chain and Rac1 in the migration of polyamine-depleted intestinal epithelial cells. *Am. J. Physiol. Gastrointest. Liver Physiol.* **292**, G983-G995.

Rosenberg, S. S., Powell, B. L. and Chan, J. R. (2007). Receiving mixed signals: uncoupling oligodendrocyte differentiation and myelination. *Cell Mol. Life Sci.* **64**, 3059-3068.

Sanders, L. C., Matsumura, F., Bokoch, G. M. and de Lanerolle, P. (1999). Inhibition of myosin light chain kinase by p21-activated kinase. *Science* **283**, 2083-2085.

Scherer, S. S., Wang, D. Y., Kuhn, R., Lemke, G., Wrabetz, L. and Kamholz, J. (1994). Axons regulate Schwann cell expression of the POU transcription factor SCIP. *J. Neurosci.* **14**, 1930-1942.

Sobue, G. and Pleasure, D. (1984). Schwann cell galactocerebroside induced by derivatives of adenosine 3′,5′-monophosphate. *Science* **224**, 72-74.

Syed, N., Reddy, K., Yang, D. P., Taveggia, C., Salzer, J. L., Maurel, P. and Kim, H. A. (2010). Soluble neuregulin-1 has bifunctional, concentration-dependent effects on Schwann cell myelination. *J. Neurosci.* **30**, 6122-6131.

Taveggia, C., Zanazzi, G., Petrylak, A., Yano, H., Rosenbluth, J., Einheber, S., Xu, X., Esper, R. M., Loeb, J. A., Shrager, P. et al. (2005). Neuregulin-1 type III determines the ensheathment fate of axons. *Neuron* **47**, 681-694.

Togo, T. and Steinhardt, R. A. (2004). Nonmuscle myosin IIA and IIB have distinct functions in the exocytosis-dependent process of cell membrane repair. *Mol. Biol. Cell* **15**, 688-695.

Totsukawa, G., Yamakita, Y., Yamashiro, S., Hartshorne, D. J., Sasaki, Y. and Matsumura, F. (2000). Distinct roles of ROCK (Rho-kinase) and MLCK in spatial regulation of MLC phosphorylation for assembly of stress fibers and focal adhesions in 3T3 fibroblasts. *J. Cell Biol.* **150**, 797-806.

Totsukawa, G., Wu, Y., Sasaki, Y., Hartshorne, D. J., Yamakita, Y., Yamashiro, S. and Matsumura, F. (2004). Distinct roles of MLCK and ROCK in the regulation of membrane protrusions and focal adhesion dynamics during cell migration of fibroblasts. *J. Cell Biol.* **164**, 427-439.

Trapp, B. D., Kidd, G. J., Hauer, P., Mulrenin, E., Haney, C. A. and Andrews, S. B. (1995). Polarization of myelinating Schwann cell surface membranes: role of microtubules and the trans-Golgi network. *J. Neurosci.* **15**, 1797-1807.

Wadgaonkar, R., Nurmukhambetova, S., Zaiman, A. L. and Garcia, J. G. (2003). Mutation analysis of the non-muscle myosin light chain kinase (MLCK) deletion constructs on CV1 fibroblast contractile activity and proliferation. *J. Cell Biochem.* **88**, 623-634.

Wang, H., Tewari, A., Einheber, S., Salzer, J. L. and Melendez-Vasquez, C. V. (2008). Myosin II has distinct functions in PNS and CNS myelin sheath formation. *J. Cell Biol.* **182**, 1171-1184.

Wolf, R. M., Wilkes, J. J., Chao, M. V. and Resh, M. D. (2001). Tyrosine phosphorylation of p190 RhoGAP by Fyn regulates oligodendrocyte differentiation. *J. Neurobiol.* **49**, 62-78.

Xu, J., Gao, X. P., Ramchandran, R., Zhao, Y. Y., Vogel, S. M. and Malik, A. B. (2008). Nonmuscle myosin light-chain kinase mediates neutrophil transmigration in sepsis-induced lung inflammation by activating beta2 integrins. *Nat. Immunol.* **9**, 880-886.

Yin, X., Kidd, G. J., Wrabetz, L., Feltri, M. L., Messing, A. and Trapp, B. D. (2000). Schwann cell myelination requires timely and precise targeting of P(0) protein. *J. Cell Biol.* **148**, 1009-1020.

Yuen, T., Wurmbach, E., Pfeffer, R. L., Ebersole, B. J. and Sealfon, S. C. (2002a). Accuracy and calibration of commercial oligonucleotide and custom cDNA microarrays. *Nucleic Acids Res.* **30**, e48.

Yuen, T., Zhang, W., Ebersole, B. J. and Sealfon, S. C. (2002b). Monitoring G-protein-coupled receptor signaling with DNA microarrays and real-time polymerase chain reaction. *Methods Enzymol.* **345**, 556-569.

Zalfa, F., Eleuteri, B., Dickson, K. S., Mercaldo, V., De Rubeis, S., di Penta, A., Tabolacci, E., Chiurazzi, P., Neri, G., Grant, S. G. et al. (2007). A new function for the fragile X mental retardation protein in regulation of PSD-95 mRNA stability. *Nat. Neurosci.* **10**, 578-587.

Zanazzi, G., Einheber, S., Westreich, R., Hannocks, M. J., Bedell-Hogan, D., Marchionni, M. A. and Salzer, J. L. (2001). Glial growth factor/neuregulin inhibits Schwann cell myelination and induces demyelination. *J. Cell Biol.* **152**, 1289-1299.

Ultrastructural characterization of myelinating cocultures abnormalities

	shCTRL	shMLCK
Total # of myelin profiles	60	31[+]
Normal profiles	49 (82%)	17 (55%)
Abnormal profiles	11 (18%)	14 (45%)[¶]
Inclusion bodies and/or myelin ovoids	6 (10%)	5 (16%)
Outpocketing and/or myelin whorls	7 (12%)	6 (19%)
Compaction defects*	0 (0%)	5 (16%)
Thin or uneven myelin*	2 (3%)	7 (23%)
SC with swollen ER*	1(2%)	4 (7%)

A total of 55 (shCTRL) and 74 (shMLCK) high magnification fields (10,500X) were scored for the presence of myelin. Cultures treated with shMLCK had significantly less myelinated axons (+) with a larger proportion of them exhibiting various morphological defects (¶). Some abnormalities (*) such as thin myelin and swollen ER were more commonly found in shMLCK cultures, while compaction defects were seen only in shMLCK-treated cultures.